Optik 156 (2018) 886–890

Contents lists available at ScienceDirect

Optik

journal homepage: www.elsevier.de/ijleo

Original research article

Effect of stirring time on the structural parameters of nanophotonic $LiNbO_3$ deposited by spin-coating technique

Y. Al-Douri[a,b,*], M.A. Fakhri[c], N. Badi[d,e], C.H. Voon[c]

[a] Nanotechnology and Catalysis Research Center (NANOCAT), University of Malaya, 50603 Kuala Lumpur, Malaysia
[b] Physics Department, Faculty of Science, University of Sidi-Bel-Abbes, 22000 Algeria
[c] Institute of Nano Electronic Engineering, University Malaysia Perlis, 01000 Kangar, Perlis, Malaysia
[d] Department of Physics, Renewable Energy Laboratory, University of Tabuk, P.O. Box 741, Tabuk 71491, Saudi Arabia
[e] Center for Advanced Materials, University of Houston, Houston, TX 77204-5004, USA

ARTICLE INFO

Article history:
Received 24 April 2017
Accepted 14 December 2017

Keywords:
Lithium Niobate
Structural properties
Spin-coating

ABSTRACT

Lithium niobate ($LiNbO_3$) photonic crystals are deposited on quartz substrate by using spin coating technique. The mixture is prepared with different stirring time (8 h, 24 h, 48 h). The $LiNbO_3$ nanostructures are analyzed by X-ray diffraction. The results show that as mixing time increases, the XRD starts to become structurallymore regular and high crystallization, therefroe it is found that the best mixing time was 48 h related to ideal syntheiss. The effect of different annealing temperatures (400, 500, and 600 °C) on the structural properties is elaborated studied towards finding ideal conditions for the preparation of optical waveguides.

1. Introduction

Lithium Niobate (LN) is a very important optical material, which is widely used by the photonics industry, mainly due to its excellent electro/acousto-optical properties [1]. LN is also an important ferroelectric material, because of its excellent piezoelectric, electro optical, pyroelectrical, and photo-refractive properties [2]. It is widely used as a polar material for photonic applications [3]. In addition, it is employed in nonlinear optics for frequency conversion and telecommunication for electro-optic modulation [4]. It is a very attractive material for the fabrication of optical waveguide devices [5,6]. It is promising for optical devices due to its mechanical robustness, good availability, optical homogeneity [7], integrated optics with lasers, modulators [8], and filters on a single LN wafer [9]. Nanophotonic $LiNbO_3$ has been studied for use in integrated form with unique pyroelectric, piezoelectric [10] and nonlinear optical properties, which would make it an ideal material for the fabrication of surface acoustic wave (SAW) [11], optoelectronic and optical devices [12,13]. LN photonic crystal was prepared using various techniques such as sputtering [14], liquid phase epitaxial (LPE) [15], metal organic chemical vapor deposition (MOCVD) [16], soft- chemistry [17], hydrothermal methods [18], and pulsed laser deposition (PLD) [19].

This work reports on the production of $LiNbO_3$ nano and micro photonic crystal by using spin-coating technique. The phase evolution with the Molar concentration was studied by using XRD; it is an important part of our work in seeking applicability of $LiNbO_3$ nano and micro photonics in optical waveguides. We have looked at the effect of stirring time of

* Corresponding author at: Nanotechnology and Catalysis Research Center (NANOCAT), University of Malaya, 50603 Kuala Lumpur, Malaysia.
E-mail address: yaldouri@yahoo.com (Y. Al-Douri).

https://doi.org/10.1016/j.ijleo.2017.12.059
0030-4026/

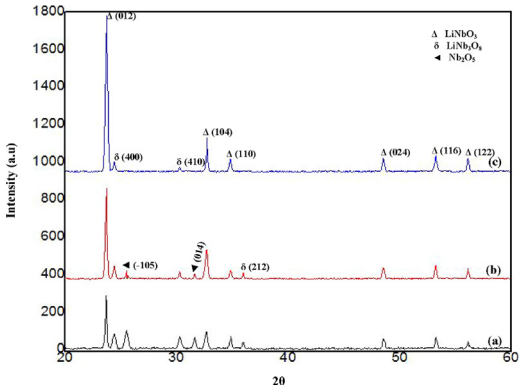

Fig. 1. XRD patterns of nanophotonic $LiNbO_3$ with different stirrer time (a) 8 h, (b) 24 h, and (c) 48 h.

mixtures used in the preparation of the nanophotonics and the effect of annealing temperature on the particles size, and structural properties, to determine the most influential on the efficiency of the photonic nanostructures in optical waveguide.

2. Experimental process

The $LiNbO_3$ nanostructures are synthesized by using Li_2CO_3 (ultra-purity, 99.99%), Ethylene Glycol (ultra-purity, 99.99%), Nb_2O_5 (ultra-purity, 99.99%), and citric acid (CA), which are purchased from Sigma Aldrich company and are used without further purification. The solution is prepared by mixing Li_2CO_3, Nb_2O_5, citric acid and Ethylene Glycol. The molar ratio between Li_2CO_3 and Nb_2O_5 was 1:1 in order to maximize the formation of $LiNbO_3$ stoichiometry phase as follow (Li_2CO_3 = 2.775 gm, Nb_2O_5 = 9.975 gm, CA = 7.875 gm and EG = 20 mm^3). First, the $LiCO_3$, Nb_2O_5, and citric acid were dissolved in Ethylene Glycol under heating and stirring conditions at 90 °C for different times i.e. 8 h, 24 h, 48 h. To obtain homogeneous and crack-free of $LiNbO_3$, the precursor was deposited by spin coating technique on quartz substrates at a spinning speed of 3000 rpm for 30 s. Seven layers were prepared and the film was dried at 120 °C for 5 min, and calcined at 250 °C for 30 min in static air and oxygen atmosphere to remove the organics, then it was annealed at 400 °C. After that we took the optimum condition of stirring time (48 h) and prepared nanostructures at different annealing temperatures; 400, 500, 600 °C. The structural evolution of the as-prepared nanostructures was examined using a high-resolution X-ray diffraction (HR-XRD), (X'Pert Pro MRD PW3040 system diffractometer, PANalytical Company, Netherlands) system equipped with Cu-Kα-radiation of wavelength λ = 0.15418 nm at 40 kV and 30 mA.

3. Results and discussion

The effect of stirring time on the XRD results of $LiNbO_3$ nanostructures deposited on quartz substrate are shown in Fig. 1. The crystalline structure of $LiNbO_3$ is found to have diffraction peaks at 2θ = 23.634, 32.637, 34.674, and 53.106 corresponding to (012), (104), (110), and (116) planes. All the diffraction peaks are indexed to the hexagonal structure with lattice parameters a = 5.145, c = 13.858, which are very close to the reported data [20]. The thin film annealed at 400 °C for 2 h in static air was polycrystalline in nature and the preferred phase was $LiNbO_3$ (Δ) phase with (012) orientation.

XRD clearly indicates the presence of a small amount of secondary Li deficient phase ($LiNb_3O_8$, δ phase) at all stirring times, at 2θ value of 24.407, 30.262 and 35.981 correspond to (400), (410) and (212) planes. This phase is originated from an interface reaction between oxygen and $LiNbO_3$. The intensity of this phase decreases as stirring time increases, and the peak which corresponds to (212) plane disappeared at stirring time, 48 h. Also, the peaks for Nb_2O_5 impurity which are observed at low stirring time at 2θ value of 24.433 and 31.623 corresponding to (−105) and (014) planes, were also not present at the stirring time, 48 h. This is due to increased number of mixing hours which increases chemical interactionsand thus improves the purity of the final mixture. The measured lattice constants have shown good agreement with experimental values as given in Table 1 [21,22]. Crystallite size (D) was calculated using Scherer's formula [23].

$$D = K\lambda/\beta cos\theta \tag{1}$$

where K is a constant taken to be 0.94, λ is the wavelength of X-ray used (λ = 1.54 Å), β is the full width at half maximum of XRD pattern and θ is Bragg's angle, around 26.41°.

In addition, the dislocation density (δ) and strain (ε) of nanophotonic $LiNbO_3$ were determined using the following relations [24].

$$\delta = 1/D^2 \tag{2}$$

$$\varepsilon = \beta/4tan\theta \tag{3}$$

Table 1
The nanophotonic $LiNbO_3$ parameters at 3000 rpm coating speed and annealed at 400 °C for 2 h for different stirrer time using XRD data.

Stirrer time(h)	Orientationhkl	Peak (θ)	Particlesize (nm)	Dislocation density(δ) (10^9) (lines/m^2)	Strain(10^{-3})	d_{hkl}(Å)	Lattice constants(Å)
8	012	23.709	100.213	9.957	1.758	3.748	a = 5.1566 c = 13.85
	104	32.701	111.105	8.292	2.516	2.735	a = 5.1566 c = 13.85
	110	34.824	93.393	11.465	2.353	2.573	a = 5.1566 c = 13.85
	024	48.516	98.680	10.269	1.092	1.874	a = 5.1566 c = 13.85
	116	53.230	83.507	13.340	3.436	1.719	a = 5.1566 c = 13.85
	122	56.123	75.570	17.511	1.384	1.637	a = 5.1566 c = 13.85
24	012	23.713	85.5797	3.24	0.837	3.749	a = 5.1566 c = 13.85
	104	33.037	86.7355	3.11	0.419	2.709	a = 5.1566 c = 13.85
	110	35.187	74.2378	8.53	0.611	2.548	a = 5.1566 c = 13.85
	024	47.493	74.5689	5.03	0.254	1.913	a = 5.1566 c = 13.85
	116	54.384	65.2881	4.278	0.559	1.686	a = 5.1566 c = 13.85
	122	56.544	63.1606	1.864	0.340	1.626	a = 5.1566 c = 13.85
48	012	23.690	68.525	2.914	0.639	3.752	a = 5.1566 5.1561[a] 5.49340[b] c = 13.85 13.8669[a]
	104	33.022	64.1833	2.971	0.359	2.710	a = 5.1566 c = 13.85
	110	35.181	59.0023	4.769	0.375	2.574	a = 5.1566 c = 13.85
	024	48.728	54.9759	4.0387	0.219	1.867	a = 5.1566 c = 13.85
	116	54.347	54.3673	5.2429	0.453	1.687	a = 5.1566 c = 13.85
	122	58.21	57.7054	1.6842	0.246	1.637	a = 5.1566 c = 13.85

[a] Ref. [21] exp..
[b] Ref. [22] exp..

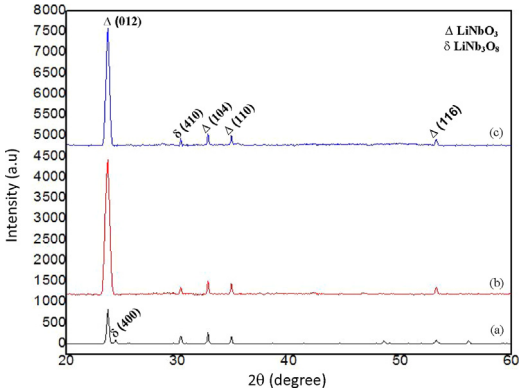

Fig. 2. XRD patterns of nanophotonic $LiNbO_3$ with different annealing temperatures (a) 400 °C, (b) 500 °C, and (c) 600 °C.

The interplanar distance (d) is calculated for all set of nanophotonic $LiNbO_3$ using Bragg's formula [24].

$$d = h\lambda/2sin\theta \tag{4}$$

Lattice constants, inter-planar angle and unit cell volumes are calculated from the lattice geometry equation [25].

$$\frac{1}{d^2} = \frac{4}{3}\left(\frac{h^2 + hk + k^2}{a^2}\right) + \frac{\iota^2}{c^2} \tag{5}$$

Fig. 1 shows nanophotonic $LiNbO_3$ with different peaks, including main diffraction for (012) plane, at different stirring times. With rising stirring time, the mean particle size decreases because the amount of stirring time leads to complete dissolution of chemical interaction and causes reduction in the particle size. The FWHM of the main peak (012) shows little higher width and higher intensity indicating an improvement of $LiNbO_3$ crystalline formation. This increases the dislocation density and strain as per Eq.(2) and Table 1.

The effect of annealing temperature on XRD results of $LiNbO_3$ nanostructures deposited on quartz substrate is shown in Fig. 2. At different temperatures:, 400, 500 and 600 °C for 2 h in static air, obtained nanostructures were polycrystalline in structure, where two phases of LN could be recognized, i.e. Δ and δ. It has been found that Δ is the preferred diffraction phase which appear at (012) orientation. Estimated value of particle size, dislocation density and strain are found to have their lowest values at 500 °C as compared to other annealing temperatures.

As annealing temperature increases, the mean particle size decreases due to restructuring and re-arrangement of crystals to improve the structural properties and to getting high purity of $LiNbO_3$ nanofilm (Δ) phase at (012) orientation. The lattice

Table 2
The nanophotonic $LiNbO_3$ parameters at 3000 rpm coating speed and strrer time 48 h with different annealing temperatures. (a) 400, (b) 500, and (c) 600 °C for 2 h using XRD data.

Annealing Temp. (°C)	Orientation hkl	Peak(2θ)	Particle size(nm)	Dislocation density(δ) (10^9) (lines/m^2)	Strain(10^{-3})	d_{hkl} (Å)	Lattice constantsa and c(Å)
400	012	23.690	88.525	3.914	0.8388	3.752	a = 5.156 c = 13.85
	104	33.022	74.183	4.971	0.5599	2.710	a = 5.156 c = 13.85
	110	35.181	79.002	5.769	0.3750	2.5736	a = 5.156 c = 13.85
	116	54.347	64.367	5.243	0.6534	1.6866	a = 5.156 c = 13.85
500	012	23.634	68.525	2.914	0.6388	3.7608	a = 5.156 5.156[a] 5.4934[b] c = 13.8513.869[a]
	104	32.637	64.183	2.971	0.3599	2.7163	a = 5.156 c = 13.85
	110	34.674	59.002	4.769	0.3750	2.5544	a = 5.156 c = 13.85
	116	53.106	54.975	4.039	0.2196	1.6904	a = 5.156 c = 13.85
600	012	23.738	57.535	5.761	1.3340	3.7533	a = 5.156 c = 13.85
	104	33.031	56.153	7.641	0.8074	2.7156	a = 5.156 c = 13.85
	110	35.224	53.868	6.683	0.7099	2.5514	a = 5.156 c = 13.85
	116	54.607	52.749	13.226	1.2876	1.6829	a = 5.156 c = 13.85

[a] Ref. [21] exp..
[b] Ref. [22] exp..

parameters of $LiNbO_3$ are calculated using Eq. (5). These parameters have no apparent changes. The dislocation density and strain are significantly influenced by the annealing temperature. However, it is very sensitive to the particle orientation and crystal structure, which may also affect the mechanical properties of the $LiNbO_3$. It can be seen that the dislocation density and strain decrease as the annealing temperature increases. As the heat treatment temperature increases up to 600 °C, the nanoparticle decomposes and as a result, both the tensile stress and strain change dramatically. The FWHM of main peak (012) shows little higher width and higher intensity as annealing temperatures increase until 500 °C then start to decline. So, improvement of the $LiNbO_3$ crystalline formation indicates the increase of dislocation density and strain as per Eq. (2) and Table 2.

The XRD clearly indicates the presence of a small amount of secondary Li deficient phase ($LiNb_3O_8$) at all of annealing temperatures with diffraction at 2θ = 30.262 corresponding to (410) plane. The measured lattice constants showed good agreement with experimental values given in Table 2. From the previous results, changes in particle size, results in inhomogenous distribution and particle size to take advantage of constructing optical waveguide.

When we want to make high efficiency optical waveguide, it is important to get a high-purity $LiNbO_3$ material, this would be possible with our results as shown in Figs. 1 and 2 where they appear to have a preference of high intensity of phase Δ to the phase δ as shown in Fig. 1. The phase Δ of Fig. 2 is also higher than that of Fig. 1. This shows the nanophotonic behavior obtained in Fig. 2 is clearer and more crystallization of nanophotonic as given in Fig. 1. Therefore, the possibility of constructing an optical waveguide could be better using parameters of Fig. 2.

4. Conclusions

Spin-coating technique was used to prepare nanophotonic $LiNbO_3$. XRD results have shown the polycrystalline nature of deposited nanophotonic $LiNbO_3$. The intensity of $LiNbO_3$ peak at 2θ = 23.634 with (012) orientation showed a significant increase as the stirring time increases, and reached a maximum of 880 for 48 h. In addition, XRD results for different annealing temperatures explain the intensity of 3500 for peak at 2θ = 23.634 with (012) orientation. The structure is more crystalline as the annealing temperature increases up to 500 °C.

References

[1] E. Marenna, C. Aruta, E. Fanelli, M. Barra, P. Pernice, A. Aronne, J. Solid State Chem. 182 (2009) 1229–1234.
[2] M. Aufray, S. Menue, Fort Y, J. Eschbach, D. Rouxel, B. Vincent, J. Nanosci. Nanotechnol. 9 (2009) 4780–4785.
[3] Ch. Fan, B. Poumellec, M. Lancry, X. He, H. Zeng, A. Erraji-Chahid, Q. Liu, Guorong Chen, Opt. Lett. 37 (2012) 2955–2957.
[4] L. Cao, A. Aboketaf, Z. Wang, S. Preble, Opt. Commun. 330 (2014) 40–44.
[5] J. Li, Dan-feng Lu, Zhi-mei Qi, Opt. Lett. 39 (2014) 3923–3926.
[6] M.A. Fakhri, Y. Al-Douri, U. Hashim, E.T. Salim, Solar Energy 120 (2015) 381–388.
[7] P. Galinetto, M. Marinone, D. Grando, G. Samoggia, F. Caccavale, A. Morbiato, M. Musolino, Opt. Laser Eng. 45 (2007) 380–384.
[8] W. Kim, S. Kwon, W. Jeong, G. Son, K. Lee, W. Choi, W. Yang, H. Lee, H. Lee, Opt. Express 17 (2009) 2638–2645.
[9] J. Guo, J. Zhu, W. Zhou, X. Huang, Opt. Commun. 294 (2013) 405–408.
[10] H. Chen, T. Lv, A. Zheng, Y. Han, Opt. Commun. 294 (2013) 202–207.
[11] H.K. Lam, J.Y. Dai, H.L.W. Chan, J. Cryst. Growth 268 (2004) 144–148.
[12] E.L. Wooten, K.M. Kissa, A. Yi-Yan, E.J. Murphy, D.A. Lafaw, P.F. Hallemeier, D. Maack, D.V. Attanasio, D.J. Fritz, G.J. McBrien, D.E. Bossi, IEEE J. Sel. Topics Quant. Electron. 6 (2000) 69–82.
[13] T. Zhang, B. Wang, Y. Zhao, S. Fang, D. Ma, Y. Xu, Mater. Chem. Phys. 88 (2004) 97–101.
[14] V. Iyevlev, A. Kostyuchenko, J. Mater. Sci. Mater. Electron. 22 (2011) 1258–1263.

[15] Y. Lu, P. Dekker, J.M. Dawes, J. Cryst. Growth 311 (2009) 1441–1445.
[16] Y. Akiyama, K. Shitanaka, H. Murakami, Y. Shin, M. Yoshida, N. Imaishi, Thin Solid Films 515 (2007) 4975–4979.
[17] M. Nyman, T.M. Anderson, P.P. Ptovenco, Cryst. Growth Des. 9 (2009) 1036–1040.
[18] R. Ageba, Y. Kadota, T. Maeda, N. Takiguchi, T. Morita, M. Ishikawa, J. Korean Phys. Soc. 57 (2010) 918–923.
[19] Y. Kang, S. Jeong, S. Lee, J. Hwang, J. Kim, C. Cho, J. Korean Phys. Soc. 49 (2006) S625–S628.
[20] A.Z. Simoes, M.A. Zaghetea, B.D. Stojanovica, C.S. Riccardi, A. Ries, A.H. Gonzaleza, J.A. Varelaa, Mater. Lett. 57 (2003) 2333–2339.
[21] A.Z. Simoes, A.H.M. González, A.A. Cavalheiro, M.A. Zaghete, B.D. Stojanovic, J.A. Varela, Ceram. Int. 28 (2002) 265–270.
[22] I.-K. Jeong, J. Korean Phys. Soc. 59 (2011) 2756–2759.
[23] Y. Al-Douri, Q. Khasawneh, S. Kiwan, U. Hashim, S.B. Abd Hamid, A.H. Reshak, A. Bouhemadou, M. Ameri, R. Khenata, Energy Convers. Manag. 82 (2014) 238–243.
[24] A. Makram, Y. Fakhri, U. Al-Douri, Evan T. Hashim, Salim, Appl. Phys. B Lasers Opt. 121 (2015) 107–116.
[25] Y. Al-Douri, A.H. Reshak, Optik 126 (2015) 5109–5114.